ADP-08-12/T672

arXiv:0811.4300v2 [hep-lat] 9 Apr 2010

Infrared exponents and the strong-coupling limit in lattice Landau gauge

André Sternbeck* and Lorenz von Smekal†
Centre for the Subatomic Structure of Matter (CSSM),
School of Chemistry & Physics, The University of Adelaide, SA 5005, Australia

(Dated: April 9, 2010)

We study the gluon and ghost propagators of lattice Landau gauge in the strong-coupling limit $\beta = 0$ in pure $SU(2)$ lattice gauge theory to find evidence of the conformal infrared behavior of these propagators as predicted by a variety of functional continuum methods for asymptotically small momenta $q^2 \ll \Lambda^2_{\rm QCD}$. In the strong-coupling limit, this same behavior is obtained for the larger values of a^2q^2 (in units of the lattice spacing a), where it is otherwise swamped by the gauge field dynamics. Deviations for $a^2q^2 < 1$ are well parameterized by a transverse gluon mass $\propto 1/a$. Perhaps unexpectedly, these deviations are thus no finite-volume effect but persist in the infinite-volume limit. They furthermore depend on the definition of gauge fields on the lattice, while the asymptotic conformal behavior does not. We also comment on a misinterpretation of our results by Cucchieri and Mendes in Phys. Rev. D81 (2010) 016005.

PACS numbers: 12.38.Gc 11.15.Ha 12.38.Aw
Keywords: strong coupling, Landau gauge, gluon and ghost propagators, infrared behavior

I. INTRODUCTION

The Green's functions of QCD are the fundamental building blocks of hadron phenomenology [1–4]. Moreover, their infrared behavior is also known to contain essential information about the realization of confinement in the covariant formulation of QCD, in terms of local quark and gluon field systems. In relation to the gluon and ghost propagators of Landau gauge QCD the Dyson-Schwinger equation studies of Refs. [5, 6] established that the gluon propagator alone does not provide long-range interactions of a strength sufficient to confine quarks, which dismissed a widespread conjecture from the 1970's going back to the work of Marciano, Pagels, Mandelstam and others. It was concluded that the infrared dominant correlations are instead mediated by the Faddeev-Popov ghosts of this formulation, whose propagator was then found to be infrared enhanced, in agreement with the Kugo-Ojima confinement criterion and thus consistent with the conditions for confinement in local quantum field theory [2, 7, 8].

This infrared behavior was subsequently confirmed by a variety of studies based on different functional methods in the continuum which all led to the same conformal infrared behavior for the gluonic Green's functions of Landau gauge QCD. These include studies of their Dyson-Schwinger Equations (DSEs) [8], Stochastic Quantization [9], and of the Functional Renormalization Group Equations (FRGEs) [10]. In fact, this conformal infrared behavior of gauge-field correlations in non-Abelian gauge theories with confinement is directly tied to the validity and applicability of the framework of local quantum field theory to such theories.

However, with the notable exception of pure $SU(2)$ lattice gauge theory in two dimensions [11], this is not what is being observed with current lattice implementations of Landau gauge [12–19]. Rather, these are much more consistent with an essentially free ghost propagator together with a massive and hence non-vanishing gluon propagator in the infrared, in qualitative agreement with DSE solutions proposed in the studies of Refs. [20–26]. Note that the functional equations of continuum quantum field theory admit both types of solutions, the *scaling solution* with the predicted conformal infrared behavior and the *decoupling solution* with a massive gluon propagator [27]. At present, the appealing aspects for fundamental reasons of the scaling solution may be seen to stand against an overwhelming evidence for the massive one, driven by the numerical results from present lattice implementations of the Landau gauge. We will review the situation briefly in the next section.

In this paper we study the gluon and ghost propagators in the strong coupling limit, $\beta \to 0$, of pure $SU(2)$ lattice Landau gauge [28, 29]. This limit can be interpreted as the limit of infinite lattice spacing, $a \to \infty$, at a fixed physical scale as set, *e.g.*, by the string tension which behaves as $a^2\sigma \propto -\ln\beta$ for $\beta \to 0$. Alternatively, when considering all momenta in lattice units, $q \sim 1/a$ as we do here, the same strong-coupling limit can also be interpreted as a hypothetic limit in which all physical momentum scales such as the string tension, $\Lambda_{\rm QCD}$ or the lowest glueball mass are sent to infinity, *i.e.*, formally as $\sigma \to \infty$ or $\Lambda_{\rm QCD} \to \infty$. Both interpretations are of course equivalent. Either way, all momenta and masses in lattice units $1/a$ are infinitely small relative to the physical scale of the theory which is precisely what we need for an analysis of the asymptotic infrared behavior of its correlation functions.

By definition, there is then no scaling limit. All momenta are zero in physical units. Having said that, we

---

*Address since October 2009: Institut für Theoretische Physik, Universität Regensburg, D-93040 Regensburg, Germany.
†Address since April 2009: Institut für Kernphysik, TU Darmstadt, Schlossgartenstr. 9, D-64289 Darmstadt, Germany.

will nevertheless distinguish large lattice momenta, with $a^2q^2 \gg 1$, from intermediate, $a^2q^2 \sim 1$, and low momenta, $a^2q^2 \ll 1$, in the strong-coupling limit. Physically, they are all in the asymptotically-far infrared, but for sufficiently large lattices, $L/a \gg 1$, only small momentum modes will be affected by finite-size corrections which can be assessed by varying the lattice size, L/a.

With this in mind, we will show that the conformal infrared behavior is indeed observed at large lattice momenta in the strong-coupling limit. Perhaps surprisingly, however, the deviations at intermediate and small momenta reveal only a negligible (though systematic) lattice-size dependence. In agreement with the standard lattice Landau-gauge simulations at finite β, we find that the small momentum behavior is well parameterized by a transverse gluon mass. This is not predominantly due to the finite volume, but it depends on the actual lattice discretization of the gauge fields, while the large momentum-behavior does not. So the latter is consistent with scaling while the data at small momenta shows decoupling, albeit being discretization dependent.

The intermediate momentum region is characterized by the transition between scaling and decoupling around $a^2q^2 \approx 1$. This transition sets a scale on an infinite lattice with $a/L \to 0$, which corresponds to a transverse gluon mass aM of the order one in the strong-coupling limit. This scale is thus not related to the string tension or glueball masses in the strong-coupling regime which all behave as $am \propto -\ln\beta$ for $\beta \to 0$. The occurance of such a new infrared scale $aM \sim 1$ seems artificial and its discretization dependence might in fact signal the breakdown of Slavnov-Taylor identities for minimal lattice Landau gauge in the strong-coupling regime.

The paper is organized as follows: In Sec. II we review the expectations for the infrared behavior from the continuum studies as background and motivation. The different parts of this section may be consulted individually or skipped on a first reading as convenient. In Sec. III we show that our numerical results for the Landau-gauge gluon and ghost propagators in the strong-coupling limit do in fact show the scaling behavior for lattice momenta with $a^2q^2 \gg 1$, that the critical exponent can be extracted in good agreement with continuum predictions from this data, and that the deviations from conformal scaling for $a^2q^2 < 1$ are well parameterized by a transverse gluon mass $M \propto 1/a$ in the infinite-volume limit. In Sec. IV we compare various lattice definitions of gauge potentials, which would all be equivalent in the continuum limit, and show that the essential features of the scaling branch at large lattice momenta, such as critical exponent and coupling, are unique. We furthermore demonstrate that the massive branch observed for $a^2q^2 < 1$ does depend on the lattice definition of the gluon fields, and that it is thus not unambiguously defined. We interpret this as an ambiguity in the definition of Landau gauge on the lattice which precludes a corresponding definition of a measure for gauge-orbit space in presence of Gribov copies [30]. One might still hope that this ambiguity will go away at non-zero β in the scaling limit. While this is true at large momenta, we demonstrate in Sec. V that the ambiguity is still present in the low-momentum region, at least for commonly used values of the lattice coupling such as $\beta = 2.3$ or $\beta = 2.5$ in $SU(2)$. Our Summary and conclusions are provided in Sec. VI and further technical details are given in two appendices.

II. INFRARED SCALING VERSUS DECOUPLING

The Landau-gauge gluon propagator, in (Euclidean) momentum space, is parameterized by a single dressing function Z,

$$D^{ab}_{\mu\nu}(p) \,=\, \delta^{ab} \left(\delta_{\mu\nu} - \frac{p_\mu p_\nu}{p^2} \right) \frac{Z(p^2)}{p^2} \;, \tag{1}$$

and the ghost propagator by a corresponding dressing function G,

$$D^{ab}_{G}(p) \,=\, -\delta^{ab} \, \frac{G(p^2)}{p^2} \;. \tag{2}$$

For their infrared behavior, *i.e.*, that of $Z(p^2)$ and $G(p^2)$ for $p^2 \to 0$, we consider the two possibilities described in the subsections that follow.

A. Scaling

The prediction of [5–10] amounts to infrared asymptotic forms

$$Z(p^2) \,\sim\, (p^2/\Lambda^2_{\mathrm{QCD}})^{2\kappa_Z} \;, \tag{3a}$$

$$G(p^2) \,\sim\, (p^2/\Lambda^2_{\mathrm{QCD}})^{-\kappa_G} \;, \tag{3b}$$

for $p^2 \to 0$, which are both determined by a unique critical infrared exponent

$$\kappa_Z = \kappa_G \equiv \kappa \;, \tag{4}$$

with $0.5 < \kappa < 1$. Under a mild regularity assumption on the ghost-gluon vertex [8], the value of this exponent is furthermore obtained as [8, 9]

$$\kappa \,=\, (93 - \sqrt{1201})/98 \,\approx\, 0.595 \;. \tag{5}$$

The conformal nature of this infrared behavior in the pure Yang-Mills sector of Landau gauge QCD is evident in the generalization to arbitrary gluonic correlations [31]: a uniform infrared limit of one-particle irreducible vertex functions $\Gamma^{m,n}$ with m external gluon legs and n pairs of ghost/anti-ghost legs of the form

$$\Gamma^{m,n} \,\sim\, (p^2/\Lambda^2_{\mathrm{QCD}})^{(n-m)\kappa} \;, \tag{6}$$

when all $p_i^2 \propto p^2 \to 0$, $i = 1, \dots 2n+m$. In particular, the ghost-gluon vertex is then infrared finite (with $n = m = 1$) as it must [32], and the nonperturbative running coupling introduced in [5, 6] via the definition

$$\alpha_s(p^2) \,=\, \frac{g^2}{4\pi} Z(p^2) G^2(p^2) \tag{7}$$

approaches an infrared fixed-point, $\alpha_s \to \alpha_c$ for $p^2 \to 0$. If the ghost-gluon vertex is regular at $p^2 = 0$, its value is [8]

$$\alpha_c \,=\, \frac{8\pi}{N_c} \, \frac{\Gamma^2(\kappa-1)\Gamma(4-2\kappa)}{\Gamma^2(-\kappa)\Gamma(2\kappa-1)} \,\approx\, \frac{9}{N_c} \times 0.99 \,. \tag{8}$$

Comparing the infrared scaling behavior of DSE and FRGE solutions of the form of Eqs. (3), it has in fact been shown that in presence of a single scale, the QCD scale Λ_{QCD}, the solution with the infrared behavior (4) and (6), with a positive exponent κ, is unique [33, 34] and nowadays being called the *scaling solution.*

B. Decoupling

This uniqueness proof does not rule out, however, the possibility of a solution with an infrared-finite gluon propagator, as arising from a transverse gluon mass M, which then leads to an essentially free ghost propagator, with the free massless-particle singularity at $p^2 = 0$, *i.e.*,

$$Z(p^2) \,\sim\, p^2/M^2 \,, \quad \text{and} \quad G(p^2) \,\sim\, \text{const.} \tag{9}$$

for $p^2 \to 0$. The constant contribution to the zero-momentum gluon propagator, $D(0) = 1/M^2$, thereby necessarily leads to an infrared constant ghost renormalization function G. This solution corresponds to $\kappa_Z = 1/2$ and $\kappa_G = 0$. It does not satisfy the scaling relations (4) or (6). This is because in this case the transverse gluons decouple for momenta $p^2 \ll M^2$, below the independent second scale given by their mass M. It is thus not within the class of scaling solutions considered above, and it is termed the *decoupling solution* in contradistinction. The interpretation of the renormalization group invariant (7) as a running coupling does not make sense in the infrared in this case, in which there is no infrared fixed-point and no conformal infrared behavior.

C. Continuum versus Lattice Studies

The functional equations of continuum quantum field theory admit two types of solutions. With the current implementations of Landau gauge on the lattice strong support is provided for the massive decoupling solution from simulations. Is this the end of the story? Superficially one might say that lattice gauge theory provides an ab initio framework whereas functional continuum methods yield ambiguous results. We would like to argue that this conclusion might be a bit premature, however. First, lattice simulations must necessarily be done in a finite volume where, strictly speaking, a conformal behavior cannot be observed, certainly not for the lowest momentum values. What is necessary to observe an at least approximate conformal behavior of the correlation functions in a finite volume of extend L, is a wide separation of scales,

$$\pi/L \,\ll p \,\ll \Lambda_{\mathrm{QCD}} \,, \tag{10}$$

such that a reasonably large number of modes with momenta p sufficiently far below the QCD scale Λ_{QCD} are accessible[1] whose corresponding wavelengths are at the same time much shorter than the finite size L.[2] Secondly, gauge-fixing in presence of Gribov copies is not so well understood on the lattice either and the relation between present implementations of lattice Landau gauge and covariant gauge theory in the continuum with local Becchi-Rouet-Stora-Tyutin (BRST) symmetry is far from clear after all [37]. Last but not least, the functional continuum methods are not as ambiguous as they might at first appear. At least technically the fact they admit both kinds of solutions is not surprising because it is well known that these methods have to be supplemented by additional boundary conditions [8, 9, 27]. It is these boundary conditions that determine which of the two solutions will be obtained, and it is essentially these boundary conditions in which the two classes of continuum studies mentioned above differ from one another. In particular, the scaling solution requires the boundary condition for the subtraction in the ghost DSE such that

$$G^{-1}(p^2) \,\to\, 0 \,, \quad \text{for}\, p^2 \to 0 \,, \tag{11}$$

which in Landau gauge then implements both, the unbroken global gauge charges of the Kugo-Ojima confinement criterion and the horizon condition of the original Gribov-Zwanziger framework [30, 38], by the infrared dominance of ghosts. This implies that the Kugo-Ojima confinement criterion cannot be derived from DSEs alone. It is implicitly implemented by the boundary condition (11) which leads to the conformal infrared behavior [8], while other choices genuinely lead to the massive one [27].

---

[1] The relevant scale here is that of the minimal MOM (MM) scheme [35]. Its relation to the $\overline{\mathrm{MS}}$ scheme, *e.g.*, for zero flavors and $N_c = 3$, with $\Lambda_{\overline{\mathrm{MS}}} \approx 240$ MeV yields $\Lambda_{\mathrm{MM}} \approx 450$ MeV. The enormous challenge for lattice simulations thus is to satisfy $\pi/L \ll p \ll 450$ MeV in the scaling region.

[2] Finite-volume effects have been analyzed carefully for the DSE scaling solution on a 4-dimensional torus which showed a quite significant volume dependence [36]. In particular, it was concluded that volumes of about 15 fm in length are needed before even an onset of the leading infrared behavior can be observed, and that up to 40 fm might be required for a reliable quantitative determination of an approximately conformal infrared behavior from a suitable range of momenta satisfying (10). That this dependence does not match up with that on a lattice became clear at the 2007 Lattice Conference, where several results were reported from large lattices [14–16], the largest for $SU(2)$ with up to 27 fm in size [15], showing practically no tendency to follow the predicted finite-size corrections to the DSE scaling solution.

More generally, from the functional equations alone (whether DSEs or FRGEs or both together) both solutions are possible, in principle. Because only the scaling solution is consistent with the conditions for confinement in local quantum field theory, based on the cohomology construction of a physical Hilbert space over the indefinite metric spaces of covariant gauge theory from BRST symmetry, this appears to be the physically relevant solution within this framework and it therefore received a lot of attention in the functional continuum studies.

The decoupling solution (9) has received renewed attention [22–26] mainly because this is what is being observed in Landau gauge implementations on the lattice [12–19]. The numerical procedures on the lattice are thereby based on minimizations of a gauge-fixing potential with respect to gauge transformations. To find absolute minima is not feasible on large lattices as this is a non-polynomially hard computational problem. One therefore settles for local minima which in one way or another, depending on the algorithm, samples gauge copies of the first Gribov region. This is mimicked in the continuum by the inclusion of Zwanziger's horizon functional to suppress the gauge copies outside the first Gribov region within the Gribov-Zwanziger framework. To make this framework compatible with the decoupling solution (9) one then introduces an additional mass term [22, 39]. While the renormalizability is maintained, one no-longer has an exact local BRST symmetry in this framework which leads to unitarity violations when attempting a BRST cohomology construction of a physical Hilbert space. This so-called soft BRST breaking only matters in the non-perturbative regime and it relates to the sampling of Gribov copies. A similar effect, in terms of reweighting copies inside and outside the first Gribov horizon, is achieved by introducing an explicit Curci-Ferrari mass [40]. In this case the reweighting is explicitly controlled by the mass and results in an explicit BRST breaking proportional to that mass. It appears that a reweighting of Gribov copies generally causes BRST breaking. At the moment it seems questionable to us whether one can have a gluon mass without reweighting of Gribov copies and BRST breaking.

Within the framework of local quantum field theory, which however requires an unbroken BRST symmetry with nilpotent BRST charge, the decoupling solution (9) is realized if and only if it comes along with the Higgs mechanism. The Kugo-Ojima confinement criterion and the infrared scaling of Landau gauge Green's functions as a consequence of this criterion cannot be dismissed from lattice simulations without a proper definition of a non-perturbative BRST symmetry. It is worth remembering, however, that the apparent ambiguity arises only when comparing the gauge dependent Green's functions of either approach. By construction, physical observables remain of course unaffected by this problem with BRST in minimal lattice Landau gauge. One example is the Polyakov-loop potential of the pure gauge theory whose center symmetry can be used to define an alternative confinement criterion which is in fact satisfied by the decoupling solution as well [41], regardless of the realization of BRST symmetry.

The agreement between lattice Landau gauge and continuum (decoupling) results, *i.e.*, when the restriction to the first Gribov region is implemented, seems quite convincing. The fact that the accuracy and conclusiveness of lattice results together with our understanding of the functional methods based on local quantum field theory have unveiled the conflict between the observed dynamical gluon mass and BRST symmetry is a great achievement. We believe that it will eventually allow us to understand the relation between Gribov copies and BRST symmetry.

Meanwhile, the strong-coupling limit of lattice Landau gauge provides a powerful tool to study this ambiguity. In this unphysical limit, the gluon and ghost correlations are solely driven by what should correspond to a non-perturbative measure of gauge-orbit space in the Landau gauge, *i.e.*, the gauge-fixing and Faddeev-Popov parts of the lattice measure. It is this measure that is being assessed when the gauge-field dynamics is switched off.

Ghost dominance, the essential condition for the conformal infrared behavior, is then implemented by hand, and if there is such a behavior, it should be seen at least in this limit in which all momenta are asymptotically small (in physical units). Because the strong-coupling limit can be interpreted as the formal limit $\Lambda_{\mathrm{QCD}} \to \infty$, it is particularly well suited to assess whether the conformal behavior of the scaling solution is seen for the larger lattice momenta, with $a^2q^2 \gg \pi^2a^2/L^2$ and thus well clear of finite-size effects, after the upper bound in (10) has been removed. This range of lattice momenta would otherwise be dominated by the dynamics due to the gauge action whose presence thus obscures any potentially conformal behavior there. As we demonstrate below, its removal does in fact reveal a scaling behavior (3), (4) for the first time in lattice simulations, and it furthermore allows to study the corrections to scaling from finite-volume effects on reasonably small lattices with some systematics.

It follows unambiguously from this study that finite-volume effects play a minor role, however, and that up to these small effects, decoupling is observed at small lattice momenta $a^2q^2 \ll 1$, with a mass parameter $M \propto 1/a$. But the strong-coupling limit also serves to isolate a discretization ambiguity which manifests itself in dependences on the lattice definition of gauge fields underlying the respective lattice Landau gauges and their measures. While this noticeably affects the decoupling branch at $a^2q^2 < 1$, the critical exponent and coupling of the scaling branch at large a^2q^2 are rather insensitive to the discretization.[3]

---

[3] Note, however, that the extraction of a scaling exponent from the

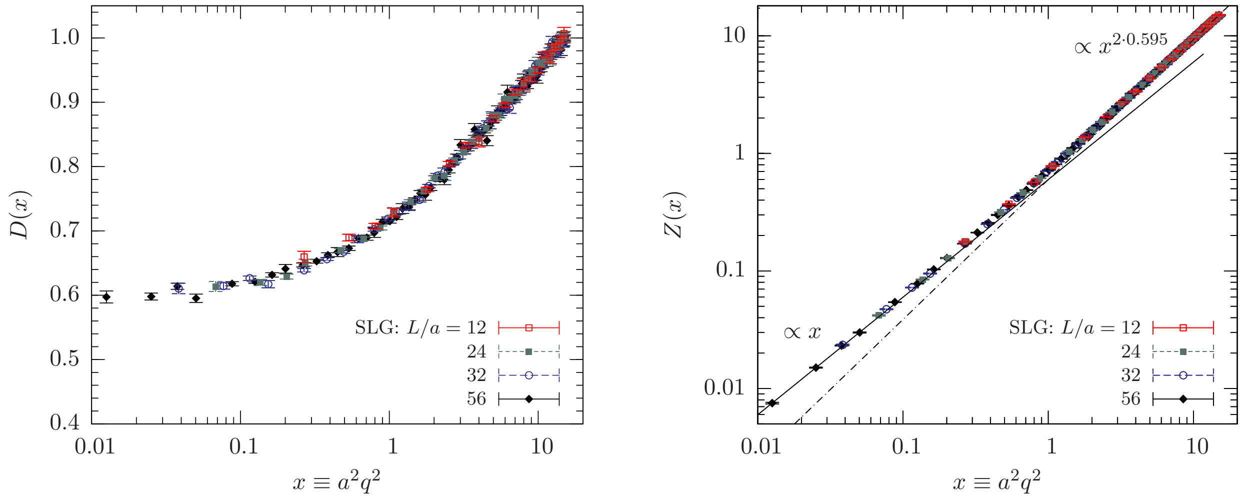

FIG. 1: The gluon propagator (left) and its dressing function Z (right) versus lattice momentum $x \equiv a^2q^2$ for different lattice sizes in the strong-coupling limit. For illustration purposes the data for Z (right) is compared to the continuum predictions from decoupling (solid) and scaling (dashed) in infinite-volume limit. That is, the respective exponents have not been fitted but set to the expected decoupling and scaling values $\kappa = 0.5$ and $\kappa \approx 0.595$.

III. STRONG-COUPLING LIMIT OF STANDARD LATTICE LANDAU GAUGE

We simulate pure $SU(2)$ gauge theory in the strong-coupling limit by generating random link configurations $\{U\}$. These are sets of $SU(2)$ gauge links,

$$U_{x\mu} = u^0_{x\mu}\mathbf{1} + i\sigma^a u^a_{x\mu}\,, \tag{12}$$

equally distributed over $(u^0, \vec{u})_{x\mu} \in S^3$. Those configurations are then fixed to the standard lattice Landau gauge (SLG) using an over-relaxation algorithm that iteratively minimizes the $SU(2)$ gauge-fixing functional, for SLG,

$$V_U[g] = 4\sum_{x,\mu}\left(1 - \frac{1}{2}\operatorname{tr} U^g_{x\mu}\right) \tag{13}$$

where the $U^g_{x\mu} = g_x U_{x\mu} g^\dagger_{x+\hat{\mu}}$ are the gauge-transformed links. The Landau gauge condition for the stationarity of $V_U[g]$ under gauge transformations g is given by the lattice divergence, $F_x(A^g) = \nabla^b_\mu A^g_{x\mu} = 0$, where ∇^b_μ denotes the lattice backward derivative and $A^g_{x\mu}$ is the lattice gluon field of SLG, defined by

$$A^g_{x\mu} = \frac{1}{2ia}\left(U^g_{x\mu} - U^{g\,\dagger}_{x\mu}\right) \tag{14}$$

in terms of the gauge-transformed link $U^g_{x\mu}$. To implement the minimal Landau gauge with a sufficient accuracy the over-relaxation algorithm is iterated until the stopping criterion

$$\varepsilon := \max_x\ \operatorname{tr}\left[(\nabla^b_\mu A^g_{x\mu})(\nabla^b_\mu A^{g\,\dagger}_{x\mu})\right] < 10^{-13} \tag{15}$$

is satisfied for every site on the lattice. Gluon and ghost propagators are then calculated in momentum space employing standard techniques. The dressing functions, Z and G, are extracted from the known tree-level form [Eqs. (A6) and (A11)] of the respective lattice propagator, see Appendix A for further details.

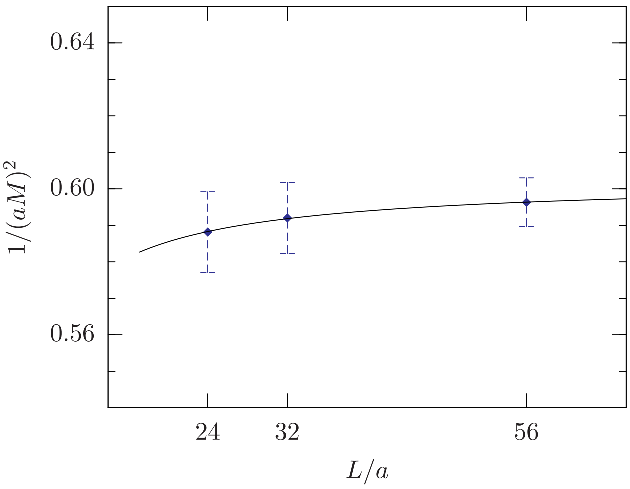

FIG. 2: The zero-momentum limit (17) of the strong-coupling gluon propagator over L/a from global fits of the form (18c).

---

ghost propagator is affected by the Gribov ambiguity as shown in the follow-up study of Ref. [42].

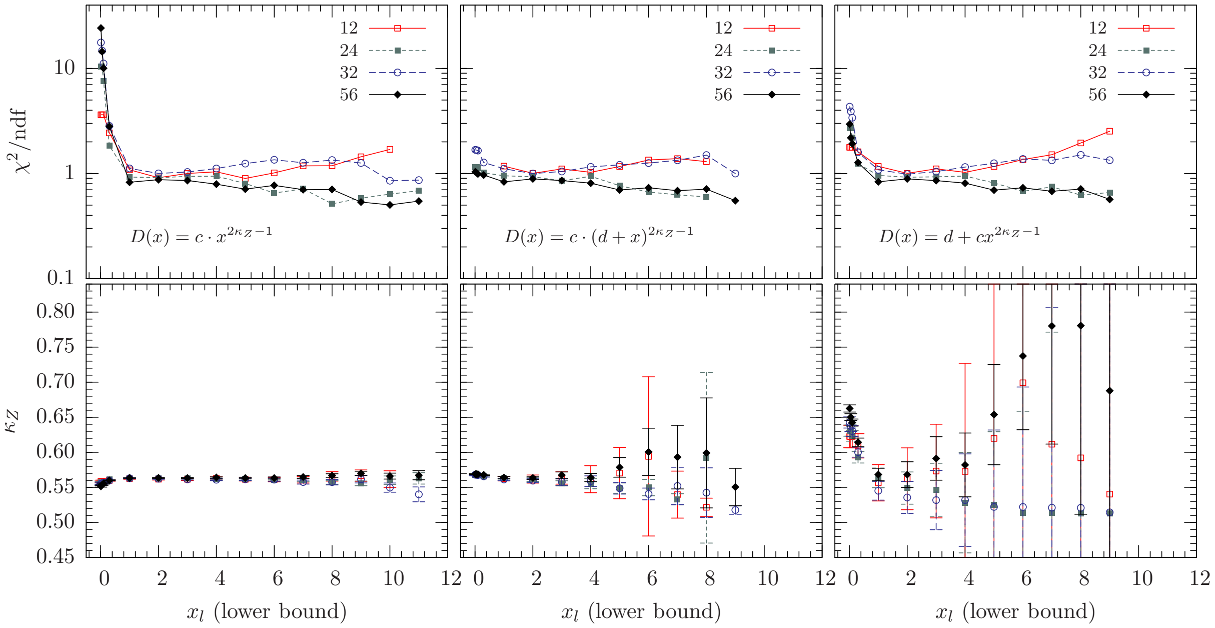

FIG. 3: χ^2/ndf and κ_Z values of fits to the gluon propagator data for different lattice sizes and different lower bounds x_l. The upper bound $x_u = 14$ has been kept fixed. The respective fit functions are given in the upper panels.

A. Gluon propagator

In Fig. 1 the data for the gluon propagator,

$$D(x) \equiv Z(x)/x\,, \quad \text{with } x \equiv a^2q^2\,, \tag{16}$$

and its dressing function Z are plotted against the lattice momenta a^2q^2 defined in Eq. (A7). The propagator is observed to increase with momentum, while it plateaus at low momenta. Perhaps unexpectedly, however, this happens irrespective of the lattice size ($N = L/a$) at around $a^2q^2 \approx 1$. It is therefore not primarily due to the finite volume. Rather, on sufficiently large lattices the observed mass behaves as

$$M^2 \equiv \lim_{x\to 0} D^{-1}(x) \propto 1/a^2 \tag{17}$$

in the strong-coupling limit with hardly any significant dependence on L. In particular, if there is a systematic L dependence at all, the zero momentum limit of the gluon propagator tends to slowly increase with the volume as shown in Fig. 2. It certainly extrapolates to a finite value $\propto 1/a^2$ in the limit $L/a \to \infty$.

In the right panel of Fig. 1 we furthermore compare the strong-coupling data for the gluon dressing function Z, to the predicted forms corresponding to decoupling (9), with $Z_\mathrm{d}(x) = c_\mathrm{d}x$, and scaling (3a), with $Z_\mathrm{s}(x) = c_\mathrm{s}x^{2\kappa_Z}$ where the value of κ_Z is not fitted but taken from Eqs. (4) and (5), $\kappa_Z = 0.595$, for comparison.

With c_d and c_s appropriately adjusted to the 56^4 data, we find that the decoupling solution provides a very good description of the low momentum region, while the large momentum branch approaches the scaling solution with an exponent κ_Z clearly above 0.5 (the fitting procedure described below leads to a conservative estimate of about $\kappa_Z = 0.57(1)$ for the 56^4 lattice, for example).

In order to assess the asymptotic form at large lattice momenta $x = a^2q^2$ more quantitatively, we have fitted the gluon propagator data to the following three forms:

$$D_a(x) = cx^{2\kappa_Z - 1}\,, \tag{18a}$$

$$D_b(x) = cx^{2\kappa_Z - 1} + d\,, \tag{18b}$$

$$D_c(x) = c(d + x)^{2\kappa_Z - 1}\,. \tag{18c}$$

D_a describes pure scaling with an effective exponent while D_b and D_c accommodate the transition between decoupling at small x and scaling at large x in different ways. In order to analyze the scaling exponent κ_Z we have used all three forms to fit the data in various windows with increasing lower bound x_l. The results are fairly insensitive to variations of the upper bound x_u in some range sufficiently close to the maximum value of $x = 16$. We used $x_u = 14$ in all fits.

The results of these fits for κ_Z as functions of the lower bound x_l with the corresponding χ^2/ndf are summarized in Fig. 3. The pure scaling model $D_a(x)$ in (18a) cannot describe the full momentum range but leads to good and stable fits to the data for $x_l \gtrsim 1$, the form $D_c(x)$ in (18c) provides the best global description of the data over the full momentum range. For x_l between 1 and 3 the results for κ_Z from all three models are consistent with each other within errors and all with χ^2/ndf of around 1. The values of κ_Z that result for the different lattice sizes from all three fit models with $x_l = 1$ are shown in Fig. 4.

As before, these values show very little systematic dependence on L/a. A slight tendency to drift towards

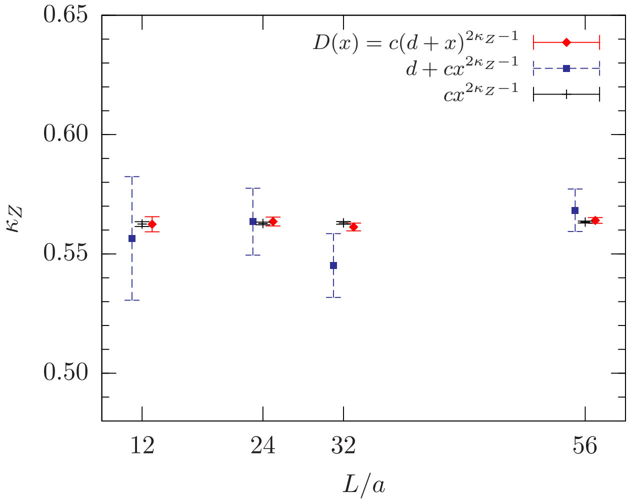

FIG. 4: The infrared exponent κ_Z for lattice sizes $L/a = 12$, 24, 32 and 56 as obtained from the strong-coupling gluon data on $x \in [1, 14]$ with the three different fit models in (18).

larger values in larger volumes is observed, but this might not be a significant effect. Assuming that there is no lattice size dependence to fit the values from model $D_c(x)$ in (18c) for the 4 different lattice sizes by a constant yields an average of $\kappa_Z = 0.563(1)$, consistent with a global average over all values in Fig. 4, while the 56^4 data alone with the same model gives $\kappa_Z = 0.564(1)$. For comparison, model $D_b(x)$ in (18b), with the largest errors, for the 56^4 data on $x \in [1, 14]$ yields $\kappa_Z = 0.568(9)$.

B. Ghost dressing function

We performed similar fits to extract the exponent κ_G from the strong-coupling ghost dressing function G as shown in Fig. 5. Those fits are less robust with a more pronounced systematic uncertainty due to the fit model dependence. This is mainly because of the wider transition region, from $G = \text{const.}$ at small x to $G \sim x^{-\kappa_G}$ at large x, which is under less control here. In fact, a pure power law is at best observed only for the very largest values of the lattice momentum, in the range above $x \approx 10$ or so. We again used three different fit models analogous to those for the gluon data in (18), one describing pure scaling at large lattice momenta and two that interpolate between decoupling (9) and scaling (3b). This time, however, we fit the inverse of the ghost dressing function G as follows:

$$G_a^{-1}(x) = cx^{\kappa_G}\,, \tag{19a}$$

$$G_b^{-1}(x) = cx^{\kappa_G} + d\,, \tag{19b}$$

$$G_c^{-1}(x) = c(d+x)^{\kappa_G}\,. \tag{19c}$$

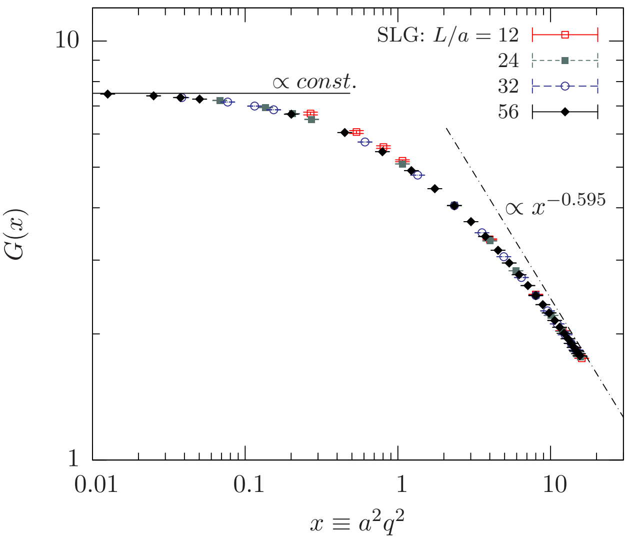

FIG. 5: The ghost dressing function G for different lattice sizes in the strong-coupling limit compared to the continuum predictions from decoupling (solid) and scaling (dashed) with the exponent from Eq. (5) in infinite-volume limit (not fitted).

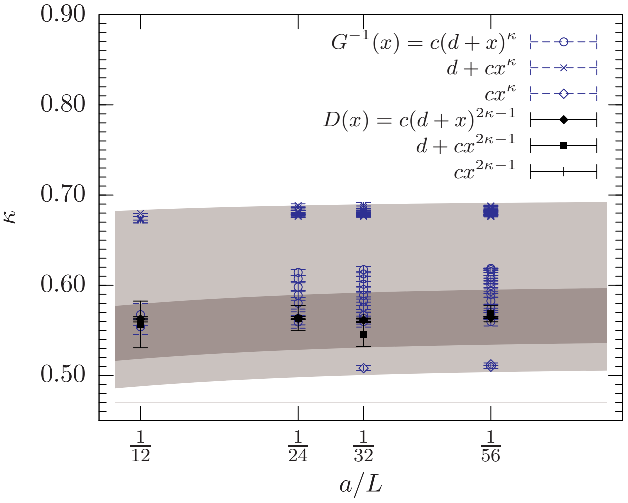

FIG. 6: κ versus a/L for the ghost and gluon propagators. Grey-colored bands mark the variation of κ with the fit model and fitting window for either propagator.

With the same method as used above, the pure scaling form G_a with lower bounds x_l around 12 leads to values of κ_G around 0.52 for the 56^4 lattice with a tendency to further increase with x_l, whereby the χ^2/ndf decrease. But the quality of those fits is still rather poor indicating that an asymptotic scaling cannot be isolated from the transition region in the ghost renormalization function.

The fit models (19b) and (19c) take this transition region better into account. The values for κ_G from G_b in (19b) are the most stable ones but tend to be rather large with κ_G around 0.68. Model G_c leads to exponents κ_G most consistent with the scaling relation in Eq. (4), with κ_G in a range between 0.55 and 0.62 depending on x_l.

The results for both exponents, κ_Z and κ_G, are summarized in Fig. 6. For the gluon exponent κ_Z these are the same data points as in Fig. 4 with the dark grey band indicating the errors and systematic uncertainties due to the fit model. The κ_G values are shown for a variety of lower bounds x_l as just described with model (19c) overlapping the gluon results. The light grey band in Fig. 6 indicates the considerably larger uncertainties in the ghost exponent, which are mainly the systematic ones due to the particular difficulty in modelling the wide transition region between decoupling and scaling there.

Nevertheless, the set of all values extracted for κ_G from the 56^4 data center around $\kappa_G = 0.60(8)$ which includes the range for the gluon exponent and is thus fully consistent with the scaling relation $\kappa_Z = \kappa_G$ in Eq. (4).

IV. DIFFERENT GAUGE-FIELD DEFINITIONS ON THE LATTICE

Strong-coupling configurations are very rough with links distributed uniformly over the parameter space, the 3-sphere for $SU(2)$. The strong-coupling limit is therefore an ideal testbed for different lattice definitions of gauge-fields which correspond to different choices of coordinates that agree only near the identity, or in the continuum limit. The standard definition (14) for example corresponds to choosing separate coordinates for the Northern (NH) and Southern Hemispheres (SH) of S^3 in the case of $SU(2)$. Strictly speaking, the SLG gluon propagator therefore corresponds to an average for each link of the contributions from NH and SH to the expectation value in Eq. (A5).

The maximal chart is provided by stereographic projection which covers the whole sphere except for the South Pole. A definition of $SU(2)$ gauge fields on the lattice based on stereographic projection is possible as follows,

$$\widetilde{A}_{x\mu} = \frac{1}{2ia}\left(\widetilde{U}_{x\mu} - \widetilde{U}^{\dagger}_{x\mu}\right) , \tag{20}$$

where

$$\widetilde{U}_{x\mu} \equiv \frac{2}{1+\frac{1}{2}\,\mathrm{tr}\,U_{x\mu}}\, U_{x\mu} . \tag{21}$$

It agrees with the standard definition near the North Pole, and in the continuum limit, but the South Pole is now at infinity and the gauge fields in (20) are thus non-compact variables. The associated Landau gauge is the *modified lattice Landau gauge* (MLG) of Ref. [43]. It follows from the stationarity condition of the modified gauge-fixing functional,

$$\widetilde{V}_U[g] = -8\sum_{x,\mu} \ln\left(\frac{1}{2} + \frac{1}{4}\,\mathrm{tr}\,U^g_{x\mu}\right) , \tag{22}$$

with respect to gauge transformations g, and reads

$$\widetilde{F}_x(A^g) = F(\widetilde{A}^g) = \nabla^b_\mu \widetilde{A}^g_{x\mu} = 0 . \tag{23}$$

When comparing MLG to the ever popular SLG, there is no advantage that the SLG has over the MLG. A promising particular feature of the MLG on the other hand is that it provides a way to perform gauge-fixed MC simulations sampling *all* Gribov copies of either sign (of the Faddeev-Popov determinant) in the spirit of BRST. This feature will be explored in a forthcoming study. Here we simply use the MLG for comparison in the standard way, *i.e.*, we gauge-fix configurations via minimization of the MLG functional in Eq. (22). The F-P operator of the MLG is given in (B7) in Appendix B.

Both lattice definitions of Landau gauge have the same continuum limit, and any differences between MLG and SLG data at finite lattice spacings are lattice artifacts. It is also worth mentioning that gauge configurations fixed to MLG do not satisfy the gauge condition of SLG and vice versa. Nevertheless, exact transversality, *i.e.*, $q_\mu(k)A_\mu(k) = 0$ or $q_\mu(k)\widetilde{A}_\mu(k) = 0$, is satisfied at finite lattice spacing a for both of them equally, with their respective Lorenz conditions $\nabla^b_\mu A_{x\mu} = 0$ or $\nabla^b_\mu \widetilde{A}_{x\mu} = 0$ and midpoint definition, if the momenta $q_\mu(k)$ are defined as $aq_\mu(k) = 2\sin(\pi k_\mu/N_\mu)$ with integer valued $k_\mu \in (-N_\mu/2, N_\mu/2]$. The identification of this so defined $q_\mu(k)$ with physical momentum is the usual tree-level correction for the Wilson gauge action. It is a special feature of MLG and SLG that their lattice Landau gauge conditions define gluon fields that are transverse in this physical momentum at any finite lattice spacing.

A. Gluon propagator

The data for the gluon propagator of SLG (red filled diamonds) is compared to that of MLG (blue filled circles) in Fig. 7. There we also show data for the gluon propagator where either

$$aA^{\mathsf{adj}}_{x\mu} = u^0_{x\mu} u^a_{x\mu} \sigma^a \quad (\text{no sum } \mu) , \tag{24}$$

or

$$aA^{\mathsf{ln}}_{x\mu} = \phi^a_{x\mu}\sigma^a/2 \quad \text{from} \quad U_{x\mu} = e^{i\phi^a_{x\mu}\sigma^a/2} \tag{25}$$

were used to define lattice gluon fields based on the adjoint representation, A^{adj} (black open diamonds), and thus blind to the center [44]; or on the tangent space at the identity A^{ln} (green crosses). In these two cases, A^{adj} and A^{ln}, for the purpose of a qualitative comparison, we simply use the gauge configurations of the SLG to calculate the gluon propagator. Especially for A^{ln} this implies, however, that the condition $q_\mu(k)A_\mu(k) = 0$ is satisfied at best approximately and nowhere near the precision of the other two (SLG and MLG). The residual uncertainty due to other possible tensor structures in the gluon propagator (A5) then causes the somewhat larger errors for this definition as seen in Figs. 7 and 8.

In Fig. 7 we have first fitted the data from all four definitions to D_c in Eq. (18c) which provides the best overall description in the full momentum range as mentioned

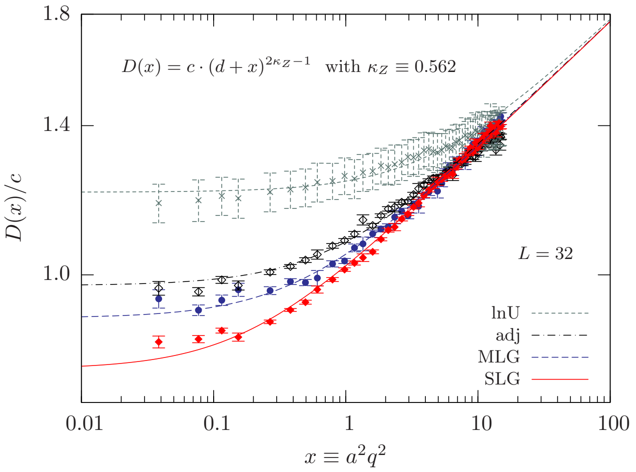

FIG. 7: The strong-coupling gluon propagator over a^2q^2 for the various definitions of gauge fields in (27). All on 32^4 lattices and normalized to the scaling branch after fitting to D_c in (18c); all with $\kappa_Z = 0.562$ from the fit to the SLG data.

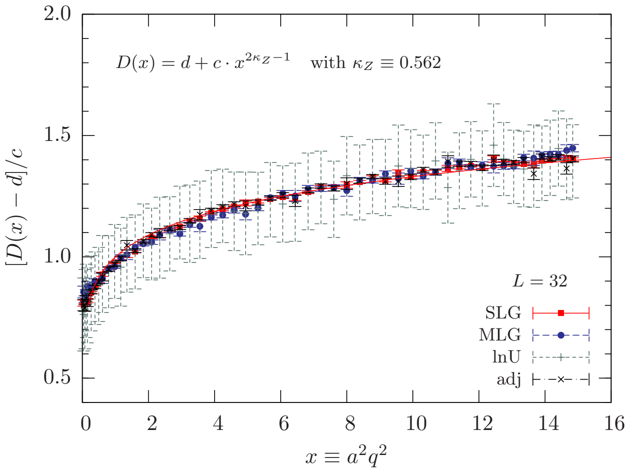

FIG. 8: Same data as in Fig. 7 but fitted to D_b in (18b) with fixed $\kappa_Z = 0.562$ and mass term subtracted in order to demonstrate how the data from all definitions then collapse onto a unique scaling curve $\propto x^{2\kappa_Z - 1}$.

above. In order to demonstrate how the other definitions compare to the SLG, we keep its value for the exponent fixed when fitting the other data, *i.e.*, $\kappa_Z = 0.562$ as obtained for $L/a = 32$ in SLG is used in all fits. Relative to the scaling branch $\propto x^{2\kappa_Z - 1}$ for large $x \equiv a^2q^2$ we then observe a strong definition dependence in the (transverse) gluon mass term at small x. The relative weight of the two asymptotic branches, scaling at large x and massive at small, is clearly discretization dependent, and this dependence cannot be compensated by finite renormalizations as is manifest in the data of Fig. 7.

The fact that the observed mass from the zero-momentum limit (17) behaves as $M \propto 1/a$ is a first indication that it is indeed this massive branch which is the ambiguous one. This is consistent with the fact that the definitions of gauge fields on the lattice, which agree at leading order, all differ at order a^2. In particular, with

$$U = \cos\frac{\phi}{2} + i\vec{\sigma} \cdot \hat{\vec{\phi}} \sin\frac{\phi}{2} \quad \text{and} \quad \vec{A} = \operatorname{tr} \vec{\sigma} A\,, \tag{26}$$

for $SU(2)$, the four different gauge field definitions (14), (20), (24) and (25) simply correspond to

$$a\vec{A} = \hat{\vec{\phi}}\, 2\sin\frac{\phi}{2} \tag{27a}$$

$$a\vec{\tilde{A}} = \hat{\vec{\phi}}\, 4\tan\frac{\phi}{4} \tag{27b}$$

$$a\vec{A}^{\mathsf{adj}} = \hat{\vec{\phi}}\, \sin\phi \tag{27c}$$

$$a\vec{A}^{\mathsf{ln}} = \vec{\phi}\,, \quad \text{with } \vec{\phi} = \hat{\vec{\phi}}\,\phi\,, \ \hat{\vec{\phi}}^2 = 1\,, \tag{27d}$$

which clearly all agree only at leading order in the limit $a \to 0$. From the order a^2 differences, the corresponding Jacobian factors lead to likewise different lattice mass counter-terms for each of the 4 definitions. This is well known from lattice perturbation theory where the lattice Slavnov-Taylor identities guarantee, however, that the gluon remains massless at every order by cancellation of all quadratically divergent contributions to its self-energy for each of the definitions. In the strong-coupling limit of minimal lattice Landau gauge, with an effective decoupling mass (9) behaving as $M^2 \propto 1/a^2$, such a contribution survives. This contribution depends on the measure for gauge fields whose definition from minimal lattice Landau gauge beyond perturbation theory is therefore ambiguous. The observation that these differences matter here explicitly demonstrates the breakdown of the lattice Slavnov-Taylor identities in minimal lattice Landau gauge in the non-perturbative domain.

To assess whether this ambiguity has an influence on the exponent κ_Z, we have also used the fits to the form D_b in Eq. (18b), again with $\kappa_Z \equiv 0.562$ fixed from the 32^4 SLG data. This fit model leads to somewhat larger χ^2/ndf arising from the transition region around $a^2q^2 \sim 1$ which this form does not describe quite as well as D_c, see the discussion in the previous section. Having obtained the fits to D_b allows us to subtract the constant d, however, which then makes the normalized data of all four definitions nicely collapse onto a unique curve $\propto x^{2\kappa_Z - 1}$ as seen in Fig. 8.

The scaling region in the strong-coupling data for the gluon propagator from all 4 definitions is fully consistent with a unique exponent κ_Z of around the SLG value with a conservative estimate of an infinite-volume extrapolation of $\kappa_Z = 0.57(3)$.

B. Ghost dressing function

Equally consistent definitions of transverse gauge-fields, gauge conditions and Faddeev-Popov operators are

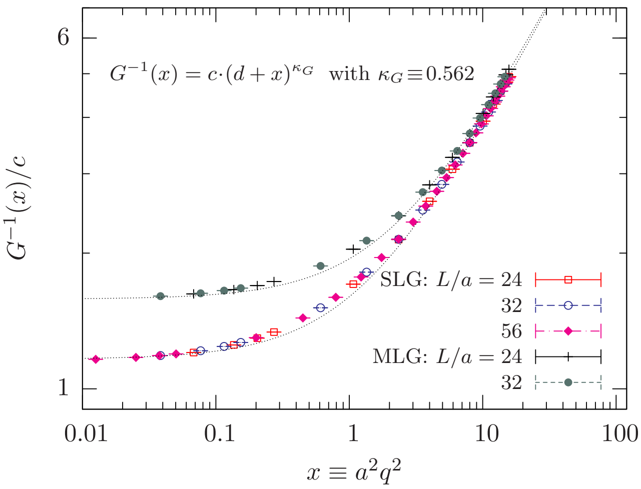

FIG. 9: Inverse ghost dressing functions in the strong-coupling limit of minimal lattice Landau gauge using standard (SLG) and modified (MLG) gauge fields/conditions.

available for SLG and MLG which allow us to compare their respective ghost propagators also. In Fig. 9 we show the strong-coupling data for the (inverse) ghost dressing functions from these two alternative definitions of lattice Landau gauge, again normalized to the scaling branch at large momenta. For this normalization we have fitted the data to model G_c in (19c) assuming the scaling relation $\kappa_G = \kappa_Z$ with the value of $\kappa_Z = 0.562$ from the 32^4 SLG gluon data. We then again observe that the two definitions approach each other in the scaling branch $\propto x^{-\kappa}$ at large x but deviate in the decoupling branch at small. Within the fit model uncertainties the ghost data from both definitions is again consistent with a unique scaling exponent, and with the scaling relation $\kappa_G = \kappa_Z$. And again the deviations in relative strengths of the two branches cannot be compensated by renormalization.

Note that in both cases, for the strong-coupling gluon and ghost propagators, the normalization constants determined from their respective scaling branches are actually not arbitrary. Their product is related to the critical coupling (8) and thus not independent but also unique as we will discuss next. This is consistent with the conclusion that it is the decoupling behavior at low momenta which is ambiguous but not the scaling behavior at large.

V. RUNNING COUPLING

The renormalization-group invariant product of Landau gauge gluon and ghost dressing functions (7) defines a running coupling. Its perturbative behavior can be determined from unrenormalized bare lattice data for the minimal Landau gauge propagators [45–47]. Its relation to the running coupling in the $\overline{\mathsf{MS}}$ scheme is known to four loops and it can provide a valuable alternative to the $\overline{\mathsf{MS}}$ coupling in phenomenological applications [35]. This furthermore permits an independent additional lattice determination of the QCD scale parameter $\Lambda_{\overline{\mathsf{MS}}}$ from continuum extrapolation of the bare product of the lattice Landau gauge propagators [45–47].

Without renormalization the bare lattice propagators are normalized so as to reproduce their respective tree-level forms [Eqs. (A6) and (A11)] for the trivial link configuration, when all links U are set to the identity element. Then, however, there is no significance in the constant prefactors of the individual propagators. This is why we removed these overall constants when comparing SLG and MLG data for these propagators individually as in Figs. 7 and 9 above. Their product (7) does not get renormalized, however, and should therefore be independent of the lattice definition used for the gauge fields up to discretization errors. We will discuss this definition independence separately in the strong-coupling limit, where the discretization effects are largest, and at finite lattice couplings β where it provides an important consistency check for the lattice determinations of the QCD scale parameter from the large momentum data of this strong running coupling as described above and in more detail in Ref. [47].

A. Strong-coupling limit

The predicted infrared scaling (3) with $\kappa_Z = \kappa_G$ immediately implies that the running coupling defined in Eq. (7) approaches an infrared fixed point, $\alpha_s \to \alpha_c$ for $p^2 \to 0$. Standard continuum conventions of course need rescaling $g^2 Z \to Z$ when comparing to lattice definitions such as (14). The predicted conformal scaling in the strong-coupling limit, with

$$Z = c_Z\,(a^2q^2)^{2\kappa} \quad \text{and} \quad G^{-1} = c_G\,(a^2q^2)^{\kappa}, \tag{28}$$

would therefore imply that the coupling (7) should be constant with

$$\alpha_s = \alpha_c = c_Z/(4\pi c_G^2)\,. \tag{29}$$

Note that its value is thus determined precisely by those multiplicative constants in the propagators that were irrelevant to the analysis in the previous section. They have to be extracted from the bare lattice data without rescaling or renormalization. Besides the critical scaling exponent κ, the critical coupling α_c is an independent additional prediction from infrared scaling and it is determined by these constants.

In complete agreement with the general observation of conformal scaling at large momenta in the strong-coupling limit, the product (7) of the gluon and ghost dressing functions levels at $\alpha_c \approx 4$ for large a^2q^2, as seen in Fig. 10. This is just below the upper bound $\alpha_c^{\max} \approx 4.46$ for $SU(2)$. The fact that α_c obtained here should be slightly smaller than this maximum value also complies with the continuum prediction in Ref. [8]: Consistent with the results of the previous section this is the

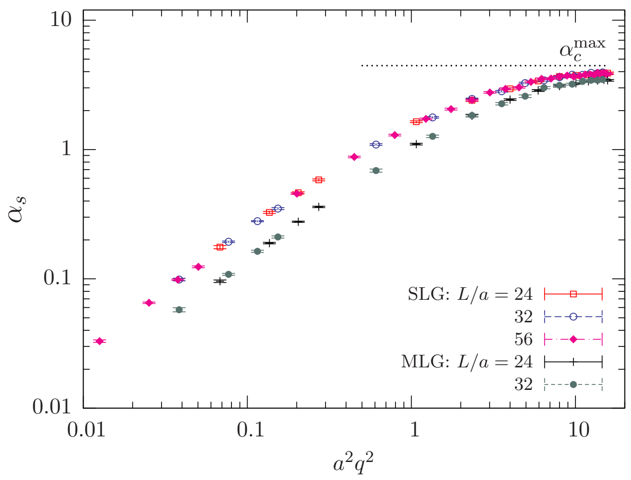

FIG. 10: The running coupling, α_s, for the standard (SLG) and modified (MLG) lattice Landau gauge at $\beta = 0$. The dotted line, $\alpha_c^{\max}$, is the critical coupling in Eq. (8) for $N_c = 2$.

expected trend for an exponent κ which is slightly smaller than the value in (5).

It is furthermore quite compelling that this result, α_c close to 4, is nearly independent of the gauge-field definition, likewise. It is almost identical for SLG and MLG, see Fig. 10. Predominantly driven by the ghost propagator, the violations to conformal infrared scaling in the form of a momentum dependence of α_s in the strong-coupling limit, set in as soon as the ambiguity in the definition of minimal lattice Landau gauge does.

B. Intermediate lattice couplings

The significant differences observed at small momenta between SLG and MLG so far were linked to the strong-coupling limit in which discretization effects are enhanced to the extreme. Even though these effects might be expected to disappear in the continuum limit, eventually, it is important to assess to what extent they survive at finite β. This is of relevance especially to the determinations of the QCD scale parameter $\Lambda_{\overline{\mathsf{MS}}}$ based on this running coupling in the perturbative domain from lattice simulations [45–47]. In particular, it is of paramount importance to verify that this ambiguity of minimal lattice Landau-gauge vanishes there, or else to find ways to include it in the estimate of the systematic uncertainties, if necessary.

As a first check, we have performed simulations in $SU(2)$ where gauge configurations were generated with the one-plaquette Wilson action at $\beta = 2.3$ and 2.5. The configurations were then fixed, as above, to SLG and to MLG, respectively, to measure and compare α_s on those two sets. For $\beta = 2.3$ the results are shown in Fig. 11. Luckily, for the α_s project mentioned above, we find no significant deviations between the two definitions at large momenta. Both agree within the statistical errors there, and the ambiguity does not appear to affect the high momentum behavior of $\alpha_s(q^2)$ as relevant to the fits of its perturbative expansion to extract the QCD scale. Of course this should nevertheless be examined more carefully as one of the possible systematic uncertainties also for the relevant $SU(3)$ configurations with dynamical quarks in future studies.

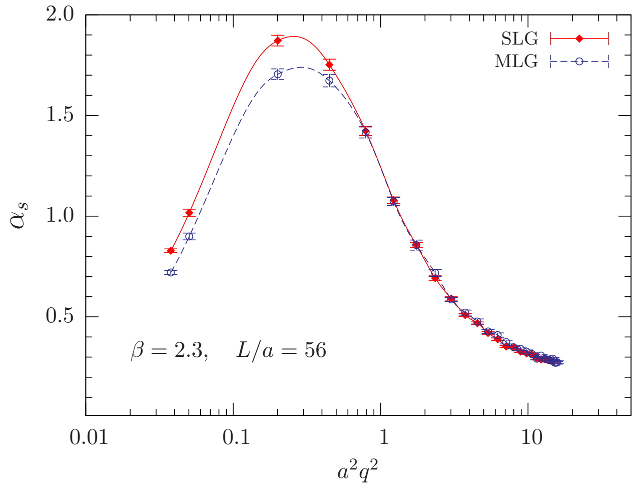

FIG. 11: Data on α_s for the standard (SLG) and modified (MLG) lattice Landau gauge at $\beta = 2.3$ using a 56^4 lattice. The lines are spline interpolations to guide the eye.

At lower momenta one observes significant differences between SLG and MLG, especially in the transition region around the maxima at $a^2q^2 \approx 0.25$. In units of the string-tension σ, with $a^2\sigma = 0.145$ for $\beta = 2.3$ from [48], this transition region corresponds to $q^2 \approx 1.7\sigma$, or with $\sigma = (440\,\mathrm{MeV})^2$, in physical units, $q \approx 570$ MeV at maximum. These observed differences persist for $\beta = 2.5$. A careful comparison of the strength of the effect for different β but comparable physical volumes, to disentangle discretization and finite-volume effects at low momenta, is left for future studies, however.

Because the Gribov copies of SLG and MLG differ, it seems quite plausible that the observed ambiguity in the minimal lattice Landau gauge beyond perturbation theory is closely related to the Gribov-copy problem. This is also suggested by our data: the effect is predominately due to the ghost propagator which is known to be affected by this problem at low momenta [42, 49–51].

VI. SUMMARY AND OUTLOOK

We have studied gluon and ghost propagators of pure $SU(2)$ minimal lattice Landau gauge theory in the strong-coupling limit. This unphysical limit probes the gauge field measure of the minimal lattice Landau gauge for there is no contribution from the Yang-Mills (plaquette) action. The Faddeev-Popov determinant is implicitly included by collapsing the gauge orbits onto the first Gribov region as sampled by the minimal Landau gauge implementation used on the lattice. The strong-coupling limit can therefore be thought of as a means to implement, by hand, a lattice analogue of the infrared dominance of ghost contributions in functional methods such as DSE or FRGE studies.

As expected in the formal limit $\Lambda_{\mathrm{QCD}} \to \infty$, it is then observed that the dressing functions of both propagators, Z and G, show the conformal scaling behavior

$$Z \propto (a^2q^2)^{2\kappa} \quad \text{and} \quad G \propto (a^2q^2)^{-\kappa}$$

for large lattice momenta, $a^2q^2 \gg 1$, well clear of the region where finite-size effects should be expected. These effects, on the other hand, turn out to be surprisingly small and the combined gluon and ghost data is consistent with an $L/a \to \infty$ extrapolation of a critical exponent $\kappa = 0.57(3)$. This scaling branch at large a^2q^2 furthermore leads to a critical coupling of $\alpha_c \approx 4$ which is just below the predicted maximum $\alpha_c^{\max} \approx 4.46$ for $SU(2)$. These results show very little if no significant dependence on the lattice definition of gauge fields and measure.

Another unambiguous result is the emergence of a transverse gluon mass $M \propto 1/a$ in the strong-coupling limit of minimal lattice Landau gauge. Both the gluon and ghost propagator show this massive behavior at small momenta corresponding to

$$Z \sim q^2/M^2 \quad \text{and} \quad G = \text{const.}$$

for $a^2q^2 \ll 1$. This massive low-momentum branch of the data, however, depends strongly on which lattice definition is being used for the gauge fields and their measure. This is typical for a mass counter-term on the lattice and demonstrates the breakdown of lattice Slavnov-Taylor identities (STIs) and BRST symmetry in minimal lattice Landau gauge beyond perturbation theory.

It is still possible that this ambiguity disappears in the continuum limit, eventually. But because it is a combination of ultraviolet (mass counter-term) and infrared (breakdown of STIs) effects, this might take very fine lattice spacings in combination with very large volumes and therefore who-knows-how big lattices to verify explicitly. As we have shown, the ambiguity is definitely present at commonly used values of the lattice couplings in $SU(2)$.

It would obviously be desirable to have a BRST symmetry on the lattice which could then provide lattice Slavnov-Taylor identities beyond perturbation theory. Non-perturbative lattice BRST has been plagued by the Neuberger 0/0 problem, but its improved topological understanding provides ways to overcome this problem [52]. It will be particularly interesting to see whether the strong-coupling behavior of the propagators will change in such approaches and whether this can lead to an unambiguous definition of lattice Landau gauge beyond perturbation theory and in the strong-coupling limit. Further studies and comparisons of different approaches to nonperturbative gauge fixing on the lattice in two and three dimensions, in particular in the strong-coupling limit will thereby be valuable next steps.

Note added in revised version

After completion of the original version of this paper, a follow-up study of the strong-coupling limit appeared [53]. There, independent data is presented for the SLG gluon and ghost propagators at $\beta = 0$ in three and four dimensions. While the four dimensional data is in complete agreement with the corresponding data presented here, the discussion of our results in [53] needs some clarification.

First, we have no intention to obscure the fact that all simulations of gluon and ghost propagators using current lattice implementations of the Landau gauge provide evidence for the qualitative low momentum behavior of the decoupling solution (9) in three and four dimensions. This includes all currently explored ranges for the lattice size L and coupling β, and our $\beta = 0$ results are no exception.

In fact, in the strong-coupling limit the scaling solution would correspond to straight lines in double-logarithmic plots as indicated by the dashed/dotted lines in Figs. 1, 5 and 10, possibly up to finite-volume corrections which would gradually disappear with increasing L/a. This is clearly not what we observe. Rather, the plateaus in the data at small lattice momenta a^2q^2 for both, the gluon propagator in Fig. 1 and the ghost dressing function in Fig. 5, are a clear indication of a massive (decoupling) behavior with almost negligible finite-volume effects as we have demonstrated.

It is nevertheless interesting, however, that we do observe for the first time on the lattice a scaling behavior (3) with a scaling exponent κ right inside the expected range, in the large momentum regime of the strong-coupling gluon propagator. This has been confirmed by the data of Ref. [53] and more recently also in [42]. The results for the ghost propagator are less conclusive but its behavior at large lattice momenta tends to approach a form consistent with the scaling relation (4), even though a clear signature for scaling over a significant range of momenta is not observed. The ghost propagator is most sensitive to the treatment of Gribov copies and thus to the nonperturbative completion of the Landau gauge. In fact, there is some recent evidence that the Gribov ambiguity can be used to tune the ghost propagator to a scaling form in the infrared [42, 54]. This would identify the one-parameter freedom in the continuum solutions to functional equations [27] as a second gauge parameter to complete the Lorenz condition nonperturbatively.

It is an unambiguous result that without this tuning the strong-coupling data for both propagators is well described by the decoupling form at small momenta in lattice units, and by scaling at large. To investigate the properties of the scaling branch at large lattice momenta, we provide three different models to fit this branch with results that are in good agreement of one another, and that give a feeling for the systematic fit-model uncertainties at the same time. In particular, the pure scaling model must fail when extending the range of the fits too far beyond the scaling branch into the small momentum region, and we see that explicitly happening in the corresponding χ^2/ndf in Fig. 3. An alternative is to define effective exponents by logarithmic derivatives and to monitor their momentum dependence [53]. This requires increased statistics but does not change the general the properties of the scaling branch and our conclusions [42]. These does not imply, however, that we suggest to dismiss the small momentum data, as we believe we were being misinterpreted in Ref. [53].

This is in contrast to the authors of Ref. [53] who write in their revised version that the data in the scaling region should be discarded. They argue that the scale $aM \sim 1$ for the transition between decoupling and scaling should be essentially given by $a\Lambda_{\rm QCD}$ and that momenta p in the scaling region therefore fail to satisfy $p \ll \Lambda_{\rm QCD}$. Even if the argument were correct, which it is not as we will explain, we would not understand why any data should be discarded. It would seem even more surprising and important to understand, if the strong-coupling limit were to show infrared scaling for momenta on the order of $\Lambda_{\rm QCD}$. Luckily that is not the case, however. Here is the flaw in the argument: The authors of [53] use a recent lattice study of the phase diagram of QCD with one flavor of staggered quarks in the strong-copuling limit [55] to assign 'physical' lengths to the lattice spacing which correspond to values of $a\Lambda_{\rm QCD}$ between 0.62 and 1.92 depending on which hadron mass or decay constant of the one-flavor strong-coupling model is being used to set the absolute scale. There is no absolute scale in the strong-coupling limit, however, not in the chiral limit of the one-flavor model, let alone in the pure gauge theory. For the latter, the relevant masses are those of the glueballs which all behave as $am \propto -\ln\beta \to \infty$ for $\beta \to 0$. It does make sense to compare mass ratios, but the relation between the absolute scale and $\Lambda_{\rm QCD}$ of the scaling region is lost at $\beta = 0$. In units of the latter, the only correct interpretation of the strong coupling limit is $a \to \infty$. The fact that the strong-coupling mesons and baryons are point-like (in lattice units) actually demonstrates that also for the quark model.

We moreover emphasize once more that the massive decoupling branch at small lattice momenta is discretization dependent. We believe that this is important and needs to be understood. It can hardly be due to violations of rotational invariance as investigated, and not surprisingly found to be very small, in [53]. Note that we did apply the usual cylinder cuts to our data in order to reduce those effects as far as possible. Moreover, we only considered lattice momenta with $a^2q^2 \leq 14$ in all our fits to the scaling branch as a further precaution. To us the observed discretization dependences signal a breakdown of Slavnov-Taylor identities in minimal lattice Landau gauge beyond perturbation theory as we explain. Maybe we are over-interpreting the strong-coupling limit which unveiled this problem, but the hope that it simply disappears in the scaling region seems overly optimistic.

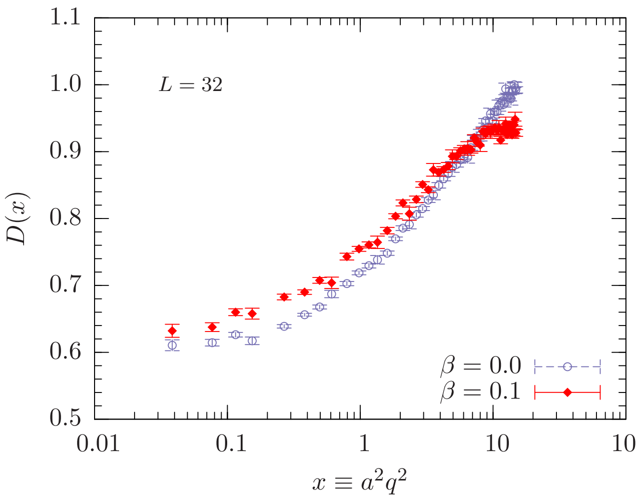

FIG. 12: The gluon propagator in lattice units versus a^2q^2 comparing data for $\beta = 0$ and $\beta = 0.1$. The $\beta = 0$ data are the same as in Fig. 1 (32^4 lattice).

The scaling properties such as exponent and coupling, on the other hand, appear to be robust under variations of the discretization of the gauge fields as far as we can judge from the available data. It is also clear, however, that the scaling branch gets suppressed as soon as the gauge action is turned back on again, as demonstrated in Fig. 12, and that one is left with the decoupling branch for low momenta at finite β. This emphasizes the importance of understanding any discretization ambiguity of the associated gluon mass, before concluding that this mass is now firmly established.

Acknowledgements

This research was supported by the Australian Research Council and by eResearch South Australia.

Appendix A: Standard lattice Landau gauge (SLG)

In this Appendix we summarize the standard approach that is nowadays widely adopted to study the gluon and ghost propagators of an SU(2) [or SU(3)] Landau gauge theory using lattice simulations. Typically, such simulations first generate a well-thermalized ensemble of gauge-invariant link configurations which then, in a second step, is fixed to what above we have called the standard lattice Landau gauge (SLG). This is most conveniently done by employing either a steepest-descent algorithm, like, e.g., the Fourier-accelerated gauge-fixing of Refs. [56, 57], or an over-relaxation algorithm [58].

Those iterative algorithms are designed to relatively fast find (for a fixed U) a set of local gauge transformations $U_{x\mu} \to U^g_{x\mu} = g_x U_{x\mu} g^\dagger_{x+\hat{\mu}}$ that minimizes the gauge functional of SLG which for the $SU(2)$ gauge group is of the form

$$V_U[g] = 4 \sum_{x,\mu} \left(1 - \frac{1}{2} \operatorname{tr} U^g_{x\mu} \right) \ . \tag{A1}$$

Any minimum of $V_U[g]$ automatically ensures that the (lattice) Landau gauge condition, *i.e.*, the lattice (backward) derivative

$$F_x(A^g) \equiv \nabla^b_\mu A^g_{x\mu} = 0 \tag{A2}$$

is satisfied if the gauge-fixed (lattice) gluon fields are given through the standard definition

$$A^g_{x\mu} = \frac{1}{2ia} \left(U^g_{x\mu} - U^{g\,\dagger}_{x\mu} \right) \tag{A3}$$

in terms of the gauge-transformed link $U^g_{x\mu}$. Practically, in order to fulfill condition (A2) with sufficient accuracy, the gauge-fixing algorithm is iterated until, e.g., the stopping criterion

$$\varepsilon = \max_x \ \operatorname{tr} \left[(\nabla^b_\mu A^g_{x\mu})(\nabla^b_\mu A^{g\,\dagger}_{x\mu}) \right] < 10^{-13} \tag{A4}$$

is satisfied for all lattice sites.

For the sake of completeness we mention that gauge functionals, like (A1), do have a huge number of different local minima. The corresponding gauge-fixed configurations do all satisfy Eq. (A2) and are related through local gauge transformations to each other. This ambiguity, known as the Gribov-copy problem on the lattice, causes minimization algorithms to find different gauge-fixed configurations all with a different value $V_U[g]$. This is, in particular, inevitable in the strong-coupling limit. The ghost propagator is known to be affected by the Gribov-copy problem while there seems to be no influence on the gluon propagator, see, e.g., Refs. [49, 50] and for $\beta = 0$ Ref. [51, 59] in particular.

To calculate the gluon propagator in momentum space, Fast Fourier transformations (FFTs) are applied transforming the gauge-fixed gluon fields $A_{x\mu} = A^a_{x\mu}\sigma^a/2$ (the superscript g is dropped in what follows) into momentum space from which the gluon propagator is then obtained for any momenta $k_\mu \in (N_\mu/2, N_\mu/2]$ as the Monte-Carlo average

$$D^{ab}_{\mu\nu}(k) = \left\langle A^a_\mu(k) A^b_\nu(-k) \right\rangle_U \tag{A5}$$

over gauge-fixed configurations U. Since for the standard Wilson gauge action the propagator's tree-level form on the lattice is of the form

$$D^{ab}_{0\,\mu\nu}(k) = \delta^{ab} \left(\delta_{\mu\nu} - \frac{q_\mu(k) q_\nu(k)}{q^2(k)} \right) \frac{1}{q^2(k)} \tag{A6}$$

where

$$q_\mu(k) = \frac{2}{a} \sin\left(\frac{\pi k_\mu}{N_\mu} \right) , \tag{A7}$$

it is natural to associate q_μ with the physical momentum. Note that then not only the continuum tensor structure of the gluon propagator is retrieved but also the gauge condition is manifest in momentum space, *i.e.*,

$$\sum_\mu q_\mu(k) A^a_\mu(k) = 0 \ . \tag{A8}$$

The gluon dressing function is straightforwardly obtained from the product $Z = q^2 D(k)$ where $D(k) = D^{aa}_{\mu\mu}(k)/9$ (summing over a and μ).

Compared to the gluon propagator, determinations of the ghost propagator

$$G^{ab}(k) = \sum_{xy} e^{ik(x-y)} \left\langle (M^{-1})^{ab}_{xy} \right\rangle_U$$

are significantly more compute intensive as they involve inversions of the Faddeev-Popov (F-P) operator M. On the lattice, M is the Hessian of the gauge functional $V_U[g]$ and for the $SU(2)$ SLG of the form

$$\begin{aligned} M^{ab}_{xy}[U_{x\mu}] = \sum_\mu \Bigg[& \left(u^0_{x,\mu} + u^0_{x-\hat{\mu},\mu} \right) \delta^{ab} \delta_{xy} \\ & - \left(u^0_{x,\mu} \delta^{ab} + \varepsilon^{abj} u^j_{x,\mu} \right) \delta_{x+\hat{\mu},y} \\ & - \left(u^0_{x-\hat{\mu},\mu} \delta^{ab} - \varepsilon^{abj} u^j_{x-\hat{\mu},\mu} \right) \delta_{x-\hat{\mu},y} \Bigg] \end{aligned} \tag{A9}$$

where we have used the same notation as in Eq. (12) and assumed periodic boundary conditions. M for the SU(3) SLG can be found, e.g., in [50].

Due to its zero eigenvalues, with corresponding constant eigenmodes, it is impossible, however, to construct the inverse of M. Nevertheless, all is not lost, as for the final analysis one is usually interested only in data of G at finite momenta for which M can be inverted on a (non-constant) vector of plane waves $\xi^a_x(c,k) = \delta^{ac} e^{2\pi ikx}$ with $k \neq 0$. Typically, the momenta k are chosen to survive both the cylinder and cone cut [60] and then $M^{ab}_{xy} \zeta^b_y(c,k) = \xi^a_x(c,k)$ is solved for $\zeta(c,k)$ yielding the ghost propagator $G^{ab}(k) = \delta^{ab} G(k)$ (directly in momentum space) where $G(k)$ is the MC average

$$G(k) = \frac{1}{3} \sum_{c=1}^{3} \left\langle \xi(k,c) \cdot \zeta(k,c) \right\rangle_U . \tag{A10}$$

In this way, also translational invariance is used to its full capacity reducing the statistical noise to a minimum.

For the inversion it is highly recommended to use a pre-conjugate gradient algorithm, e.g., that of Ref. [50]. This precondition has been proven to drastically accelerate computations, in particular, when lattices sizes are as big as we have used for this study and can also be straightforwardly applied to the case of Coulomb gauge as done, e.g., in [61, 62]. For further details on this technique refer to [63].

At tree-level the F-P operator is simply $-\delta^{ab}\Delta_{xy}$ where Δ denotes the lattice Laplacian in four dimensions. Consequently, the tree-level form of the ghost propagator on the lattice is

$$G_0^{ab}(k) = -\delta^{ab}\frac{1}{q^2(k)} \tag{A11}$$

where q_μ is that of Eq. (A7).

Appendix B: Modified lattice Landau gauge (MLG)

In this Appendix we summarize the Modified lattice Landau gauge (MLG) of Ref. [43] and provide the reader with the necessary information for the gauge group $SU(2)$ as used in Sec. IV.

The MLG is a novel implementation of the Landau gauge for lattice gauge theories which was introduced in Ref. [43] for the gauge groups $U(1)$ and $SU(2)$. It is based on stereographic projection to define lattice gauge fields and extensions to the gauge group SU(3) or to Coulomb gauge are also possible.

When comparing MLG to the ever popular SLG, there is no advantage that the SLG has over the MLG. A promising particular feature of the MLG on the other hand is that it provides a way to perform gauge-fixed MC simulations sampling *all* Gribov copies of either sign (of the Faddeev-Popov determinant) in the spirit of BRST. This is because in MLG there is no perfect cancellation of Gribov copies of opposite sign, known as the Neuberger 0/0 problem, which prevented us from performing such simulations for 20 odd years. Note that in the standard lattice approach to Landau gauge, *i.e.*, via a minimization of the SLG functional [Eq. (A1)], only Gribov copies within the first Gribov region, *i.e.*, with positive sign, are sampled. Gauge-fixed Monte Carlo simulations via MLG, however, would enable us to sample beyond that region. Indeed such simulations are not meant to compete in any sense with standard MC simulation of lattice gauge theory, as gauge-invariant observables would be completely unaffected by that, but rather to provide a theoretical sound framework for studying non-perturbative properties of gauge-variant correlation functions.

This particular feature of MLG will be explored in a forthcoming study. Here we simply have used the MLG for comparison in the standard way, *i.e.*, we gauge-fix configurations via minimization of the MLG functional,

$$\widetilde{V}_U[g] = -8\sum_{x,\mu}\ln\left(\frac{1}{2}+\frac{1}{4}\,\mathrm{tr}\,U^g_{x\mu}\right). \tag{B1}$$

Consequently, only the first Gribov region of MLG is sampled, however when doing so we are in the fortunate position of having two alternative lattice implementations of $SU(2)$ Landau gauge theory which differ at finite lattice spacing, a, but meet in the continuum limit. When comparing SLG to MLG data the impact of discretization errors can then be seen at any finite a.

Leaving aside the issue of Gribov copies, we adapt the Fourier-acceleration of Ref. [56] to gauge-transform configurations such that they satisfy the lattice Landau gauge condition, here that of MLG,

$$\nabla^b_\mu \widetilde{A}_{x\mu} = 0\,. \tag{B2}$$

This automatically maximizes the MLG functional [Eq. (B1)] when $\widetilde{A}_{x\mu}$, the lattice gluon field of MLG, is given through

$$\widetilde{A}_{x\mu} \equiv \frac{1}{2ia}\left(\widetilde{U}_{x\mu}-\widetilde{U}^\dagger_{x\mu}\right) \tag{B3}$$

where

$$\widetilde{U}_{x\mu} \equiv \frac{2U_{x\mu}}{1+\frac{1}{2}\,\mathrm{tr}\,U_{x\mu}}\,. \tag{B4}$$

In our study the Fourier-accelerated gauge-fixing is iterated until the stopping criterion

$$\max_x\ \mathrm{tr}\left[\nabla^b_\mu\widetilde{A}_{x\mu}\nabla^b_\mu\widetilde{A}^\dagger_{x\mu}\right] < 10^{-13}\,. \tag{B5}$$

is met at all lattice sites.

Note that gauge-fixed configurations satisfying Eq. (B5) do not satisfy that of SLG [Eq. (A4)] and vice versa. Nevertheless, transversality of the corresponding lattice gluon field is ensured in both cases, if momenta are associated with Eq. (A7) and the standard midpoint definition is assumed. That is,

$$\sum_\mu q_\mu(k)\widetilde{A}^a_\mu(k) = 0\,. \tag{B6}$$

The gluon propagator of MLG is straightforwardly constructed as in SLG with A substituted through $\widetilde{A}$. Similar holds for the ghost propagator, though in MLG the F-P matrix is of the form

$$\widetilde{M}^{ab}_{xy} = \sum_{\mu}\Big\{ -\Big(\tilde{u}^0_{x,\mu}\delta^{ab} + \epsilon^{abc}\tilde{u}^c_{x,\mu} + \frac{1}{2}\tilde{u}^a_{x,\mu}\tilde{u}^b_{x,\mu}\Big)\delta_{x+\hat{\mu},y} + \Big[(\tilde{u}^0_{x,\mu} + \tilde{u}^0_{x-\hat{\mu},\mu})\delta^{ab} + \frac{1}{2}\tilde{u}^a_{x,\mu}\tilde{u}^b_{x,\mu} + \frac{1}{2}\tilde{u}^a_{x-\hat{\mu},\mu}\tilde{u}^b_{x-\hat{\mu},\mu}\Big]\delta_{xy} - \Big(\tilde{u}^0_{x-\hat{\mu},\mu}\delta^{ab} - \epsilon^{abc}\tilde{u}^c_{x-\hat{\mu},\mu} + \frac{1}{2}\tilde{u}^a_{x-\hat{\mu},\mu}\tilde{u}^b_{x-\hat{\mu},\mu}\Big)\delta_{x-\hat{\mu},y}\Big\} \tag{B7}$$

where $\tilde{u}^0 = 2u^0/(1+u^0)$ and $\vec{\tilde{u}} = 2\vec{u}/(1+u^0)$. Due to the logarithm in Eq. (B1) there are $\tilde{u}^a\tilde{u}^b$-terms quadratic in the projected variables $\tilde{u}$. Apart from those, $\widetilde{M}$ is of the same form as the standard F-P operator in $SU(2)$ [Eq. (A9)] with the u's replaced by $\tilde{u}$. Therefore, the tree-level forms of the gluon and ghost propagators, Eq. (A6) and (A11), are also valid in MLG.

[1] C. D. Roberts and A. G. Williams, Prog. Part. Nucl. Phys. **33**, 477 (1994), hep-ph/9403224.

[2] R. Alkofer and L. von Smekal, Phys. Rept. **353**, 281 (2001), hep-ph/0007355.

[3] C. S. Fischer, J. Phys. **G32**, R253 (2006), hep-ph/0605173.

[4] C. D. Roberts, M. S. Bhagwat, A. Holl, and S. V. Wright, Eur. Phys. J. ST **140**, 53 (2007), 0802.0217.

[5] L. von Smekal, R. Alkofer, and A. Hauck, Phys. Rev. Lett. **79**, 3591 (1997), hep-ph/9705242.

[6] L. von Smekal, A. Hauck, and R. Alkofer, Ann. Phys. **267**, 1 (1998), hep-ph/9707327.

[7] R. Alkofer and L. von Smekal, Nucl. Phys. **A680**, 133 (2000), hep-ph/0004141.

[8] C. Lerche and L. von Smekal, Phys. Rev. **D65**, 125006 (2002), hep-ph/0202194.

[9] D. Zwanziger, Phys. Rev. **D65**, 094039 (2002), hep-th/0109224.

[10] J. M. Pawlowski, D. F. Litim, S. Nedelko, and L. von Smekal, Phys. Rev. Lett. **93**, 152002 (2004), hep-th/0312324.

[11] A. Maas, Phys. Rev. **D75**, 116004 (2007), 0704.0722.

[12] A. Sternbeck, E.-M. Ilgenfritz, M. Müller-Preussker, A. Schiller, and I. L. Bogolubsky, PoS **LAT2006**, 076 (2006), hep-lat/0610053.

[13] E.-M. Ilgenfritz, M. Müller-Preussker, A. Sternbeck, A. Schiller, and I. L. Bogolubsky, Braz. J. Phys. **37**, 193 (2007), hep-lat/0609043.

[14] A. Sternbeck, L. von Smekal, D. B. Leinweber, and A. G. Williams, PoS **LAT2007**, 340 (2007), 0710.1982.

[15] A. Cucchieri and T. Mendes, PoS **LAT2007**, 297 (2007), 0710.0412.

[16] I. L. Bogolubsky, E.-M. Ilgenfritz, M. Müller-Preussker, and A. Sternbeck, PoS **LAT2007**, 290 (2007), 0710.1968.

[17] A. Cucchieri and T. Mendes, Phys. Rev. Lett. **100**, 241601 (2008), 0712.3517.

[18] A. Cucchieri and T. Mendes, Phys. Rev. **D78**, 094503 (2008), 0804.2371.

[19] I. L. Bogolubsky, E.-M. Ilgenfritz, M. Müller-Preussker, and A. Sternbeck, Phys. Lett. **B676**, 69 (2009), 0901.0736.

[20] A. C. Aguilar and A. A. Natale, JHEP **08**, 057 (2004), hep-ph/0408254.

[21] P. Boucaud et al., JHEP **06**, 001 (2006), hep-ph/0604056.

[22] D. Dudal, S. P. Sorella, N. Vandersickel, and H. Verschelde, Phys. Rev. **D77**, 071501 (2008), 0711.4496.

[23] A. C. Aguilar, D. Binosi, and J. Papavassiliou, Phys. Rev. **D78**, 025010 (2008), 0802.1870.

[24] A. C. Aguilar, D. Binosi, and J. Papavassiliou, PoS **LC2008**, 050 (2008), 0810.2333.

[25] P. Boucaud et al., JHEP **06**, 012 (2008), 0801.2721.

[26] P. Boucaud et al., JHEP **06**, 099 (2008), 0803.2161.

[27] C. S. Fischer, A. Maas, and J. M. Pawlowski, Annals Phys. **324**, 2408 (2009), 0810.1987.

[28] A. Sternbeck and L. von Smekal, PoS **LATTICE2008**, 267 (2008), 0810.3765.

[29] A. Sternbeck and L. von Smekal, PoS **CONFINEMENT8**, 049 (2008), 0812.3268.

[30] V. N. Gribov, Nucl. Phys. **B139**, 1 (1978).

[31] R. Alkofer, C. S. Fischer, and F. J. Llanes-Estrada, Phys. Lett. **B611**, 279 (2005), hep-th/0412330.

[32] J. C. Taylor, Nucl. Phys. **B33**, 436 (1971).

[33] C. S. Fischer and J. M. Pawlowski, Phys. Rev. **D75**, 025012 (2007), hep-th/0609009.

[34] C. S. Fischer and J. M. Pawlowski, Phys. Rev. **D80**, 025023 (2009), 0903.2193.

[35] L. von Smekal, K. Maltman, and A. Sternbeck, Phys. Lett. **B681**, 336 (2009), 0903.1696.

[36] C. S. Fischer, A. Maas, J. M. Pawlowski, and L. von Smekal, Annals Phys. **322**, 2916 (2007), hep-ph/0701050.

[37] L. von Smekal (2008), 0812.0654.

[38] D. Zwanziger, Nucl. Phys. **B399**, 477 (1993).

[39] D. Dudal, J. A. Gracey, S. P. Sorella, N. Vandersickel, and H. Verschelde, Phys. Rev. **D78**, 065047 (2008), 0806.4348.

[40] L. von Smekal, M. Ghiotti, and A. G. Williams, Phys. Rev. **D78**, 085016 (2008), 0807.0480.

[41] J. Braun, H. Gies, and J. M. Pawlowski, Phys. Lett. **B684**, 262 (2010), 0708.2413.

[42] A. Maas, J. M. Pawlowski, D. Spielmann, A. Sternbeck, and L. von Smekal, Eur. Phys. J. C, in press (2010), 0912.4203.

[43] L. von Smekal, D. Mehta, A. Sternbeck, and A. G. Williams, PoS **LAT2007**, 382 (2007), arXiv:0710.2410 [hep-lat].

[44] K. Langfeld, H. Reinhardt, and J. Gattnar, Nucl. Phys. **B621**, 131 (2002), hep-ph/0107141.

[45] A. Sternbeck et al., PoS **LAT2007**, 256 (2007),

0710.2965.

[46] P. Boucaud et al., Phys. Rev. **D79**, 014508 (2009), 0811.2059.

[47] A. Sternbeck et al., PoS **LAT2009**, 210 (2009), 1003.1585.

[48] K. Langfeld, Phys. Rev. **D76**, 094502 (2007), 0704.2635.

[49] T. D. Bakeev, E.-M. Ilgenfritz, V. K. Mitrjushkin, and M. Müller-Preussker, Phys. Rev. **D69**, 074507 (2004), hep-lat/0311041.

[50] A. Sternbeck, E.-M. Ilgenfritz, M. Müller-Preussker, and A. Schiller, Phys. Rev. **D72**, 014507 (2005), hep-lat/0506007.

[51] A. Cucchieri, Nucl. Phys. **B508**, 353 (1997), hep-lat/9705005.

[52] L. von Smekal, A. Jorkowski, D. Mehta, and A. Sternbeck, PoS **CONFINEMENT8**, 048 (2008), 0812.2992.

[53] A. Cucchieri and T. Mendes, Phys. Rev. **D81**, 016005 (2010), 0904.4033.

[54] A. Maas (2009), 0907.5185.

[55] P. de Forcrand and M. Fromm, Phys. Rev. Lett. **104**, 112005 (2010), 0907.1915.

[56] C. T. H. Davies et al., Phys. Rev. **D37**, 1581 (1988).

[57] A. Cucchieri and T. Mendes, Phys. Rev. **D57**, 3822 (1998), hep-lat/9711047.

[58] J. E. Mandula and M. Ogilvie, Phys. Lett. **B248**, 156 (1990).

[59] A. Cucchieri, Phys. Lett. **B422**, 233 (1998), hep-lat/9709015.

[60] D. B. Leinweber, J. I. Skullerud, A. G. Williams, and C. Parrinello (UKQCD), Phys. Rev. **D60**, 094507 (1999), hep-lat/9811027.

[61] A. Voigt, E.-M. Ilgenfritz, M. Müller-Preussker, and A. Sternbeck, Phys. Rev. **D78**, 014501 (2008), 0803.2307.

[62] Y. Nakagawa et al., Phys. Rev. **D79**, 114504 (2009), 0902.4321.

[63] A. Sternbeck, PhD thesis (Humboldt University Berlin) (2006), hep-lat/0609016.